LASER REMELTING AS MEAN TO REDUCE CLAD MISORIETATED VOLUME DEPOSITED THROUGHT LASER CLADDING WHEN APPLIED TO SINGLE CRISTALINE TURBINE BLADES

Adriano de Souza Pinto Pereira, adriano.pereira@grad.ufsc.br[1]
Boris Rottwinkel, b.rottwinkel@lzh.de[2]
Stefan Kaierle, s.kaierle@lzh.de[2]
Walter Lindolfo Weingaertner, w.l.weingaertner@ufsc.br[1]
Volker Wesling, office@isaf.tu-clausthal.de[2]

[1]Universidade Federal de Santa Catarina, Campus Reitor João David Ferreira Lima, Florianópolis – SC
[2]Laser Zentrum Hannover e.V., Hollerithallee 8, 30419 Hannover, Alemanha

Abstract. *The work presented had as objective the simplification of the already hard-to-achieve repair of single crystalline (SX) turbine blades, a process that could significantly reduce the costs of modern aviation. The deposition of SX clads by the laser cladding process has shown promising results on this ambit and here is seen as a tool to be improved. It was assumed, that remelting could be used to extend SX-height during re-solidification of each cladded track's misoriented volume, and thus laser remelting of such clad tracks is this work's focus. All tests were performed with CMSX-4, a SX Ni-based superalloy. After remelting tests a chosen re-molten clad track was used to form higher single crystalline depositions, reaching considerable SX volumes. Tests were executed in the crystalline orientations (010)/[100] or (010)/[001]; which are equivalent to orientation commonly found during a turbine repair process. Laser remelting was proven an efficient option when aiming SX increase of repair clads.*

Keywords: *Laser Cladding, Remelting, Single Crystalline Repair, CMSX-4, Turbine Blades.*

1. INTRODUCTION

In the past decades, single crystalline (SX) nickel based superalloys began to be used on high-temperature gas turbines. This was done in order to elevate engine-working temperatures, thus improving efficiency. On such engines, from the single crystalline parts used, the most numerous are the blades with high manufacturing cost, which during their lifespan undergo erosion and cracking. At the moment, these blades do not have a fully-effective repair method. This is due to the difficulty in adding material to them while maintaining deposition single crystallinity and avoiding solidification cracks; read, maintaining the properties of the original material. A number of processes are been studied focusing such repair, being selective laser melting (SLM), laser material deposition (LMD) - and others equivalent - the ones receiving more attention. Such processes would deposit new material after the removal of the damaged volume.

Acharya et al. (2014a) presented recently a sophisticated computational model designed to predict the microstructure evolution obtained from a single SLM laser raster pass. This work followed to a methodology to couple the model with experimental data (Acharya et al., 2014b). Their research resulted in a tool with predictive capabilities regarding laser-based SX-repair processes. Now on the ambit of LMD, Liu and Qi designed a model to predict the microstructure formation of a single clad track in laser powder deposition (LPD) (Liu and Qi, 2014). Simultaneously, they studied the influence of substrate orientation in such process (Liu and Qi, 2015). Both Liu and Qi's works achieved reasonable correlation between model and the physical; and presented indicatives of the studied process variables' behaviour. More recently, but in another paper, Z. Liu et al. (2016)confirmed possible to improve LPD SX-results by inclination of the coaxial cladding nozzle used in their work.

Liu and DuPont (2004) studied the effects of melt-pool geometrical parameters on crystal growth and microstructure development during laser surface remelting of single crystalline superalloys. The process is treated there as a "powderless" laser cladding. A computational model to predict crystalline orientation based on geometrical parameters is used. The study was extended to other crystalline orientations on a following work (Liu and DuPont, 2005). In both Liu and DuPont's articles the modelling agreed with remelting experiments. Recently, Wang et al. (2015) presented recommendations regarding the crystalline orientations to be used when repairing a SX turbine blade. Their work is complementary to Liu and DuPont's. Accordingly to Wang, by rotating around [010] crystalline direction from a

(001)/[100] orientation one could push the columnar to equiaxed transition (CET) in the substrate's surface direction (Wang et al., 2015) and also reduce the probability of stray grain formation (Wang L. and Wang N., 2016).

However, earlier to the references mentioned – which had a focus turned in improving the outcomes of a specific process – researchers were more interested in understanding the solidification phenomena behind such laser repairs. Mokadem et al. (2007) was the first to propose the oriented-to-misoriented transition (OMT). This phenomenon is caused by off-heat flow axis dendrite growth and represents a major concern in controlling or modelling SX-solidification. Once that several crystalline orientations are encountered when repairing turbine blades. Vitek (2005) established the bases of stray grain formation caused by constitutional supercooling ahead of the dendritic growth front. Such was done by analysing welding conditions through a simple thermal and geometrical model and then comparing them with actual welding experiments. Gäumann et al. (1997), improved Hunt's (1984) mathematical model of the CET, one of the situations where SX-regime is broken. This model achieved better predictions at low thermal gradients and low solidification velocities. On further work, Gäumann et al. (2001) also defined the first's microstructure solidification maps for the single-crystalline laser deposition of superalloys, resulting in important recommendations to be taken when designing process conditions.

The goal of the current work is to present the achievement of high single crystalline depositions by the process of coaxial laser powder cladding – a form of LPD – when aided by laser remelting, while also studying the importance of cladding strategy in track superposition. One can see from the works listed previously that the study of LPD-derived processes is preferred. This is due to their spatial flexibility and spot-like applicability, suitable for repair of most blade defects. However, it is rather complex to attain a cladded track with great single crystallinity and even more to form a wide multi-layer SX-clad. Thus, with intention to overcome this difficulty, this work proposes to combine LPD with laser remelting. It is expected that, once re-melted, a track's crystalline misoriented volume will re-solidify, allowing it to reorient as an extension of the substrate track's overall single crystalline height. It must be also mentioned that the right conditions for epitaxial solidification must be provided and only the necessary volume should be melted, thus avoiding rework. Possible secondary benefits from remelting were also expected, as the suppression of track shape irregularities, or the reduction of residual solidification tensions resultant from cladding.

With proper remolten clad tracks at hand, the experimentation moved to study the multi-layer cladding of re-molten tracks. As a layer is the base unit of a multi-layer clad, an initial study was done in order to adjust track overlapping without impairing single crystallinity. In the next stage, the satisfactory, quasi-SX layer achieved would be repeated over itself, aiming higher cladded structure heights. The product would come to be an CMSX-4 single crystal. Evaluation of final microstructure, regarding mainly its defects and dendrite orientations, was done metallographicaly.

2. EXPERIMENTAL

As laser source a diode laser system was used, whose four diode arrays produce a continuous laser beam on TEM-00 mode. The focused beam had a 980 nm wavelength, with a maximum power of 340 W. Other laser beam characteristics at focus are: spot size diameter of 808 μm; focal distance at 200 mm; Rayleigh length of 4.71 mm; M^2 of 121.4. Regarding the substrate, the tests were executed over two millimetres thick CMSX-4 plates, with their [001] direction always considered to be the direction of the material main dendrites branch. That said, the processing passes over the substrate were performed in approximation to the (010)/[100] and (010)/[001] orientations.

The approximation was due to the nature of the samples available. They were cuboidal and although it was known through the supplier that their [001] direction was quasi-parallel to three of the sample sides, the other [100] and [010] directions were not defined. To determine the other crystalline orientations a simple method was developed. It consisted in calculating the substrate secondary dendrite arms angles in relation with the surface through optical metallography. Each CMSX-4 sample available had one of its two sides parallel to the (001) plane sandpaper-grinded through the 800, 1200, 2500 grits (ISO) and without polishing, had received an eight-minutes etching by a solution with the composition: 100 ml of distilled water; 50 ml HCl; 5 g FeCl3. Macrographs from the prepared surface were taken and the geometric relations depicted on Fig. 1 were defined.

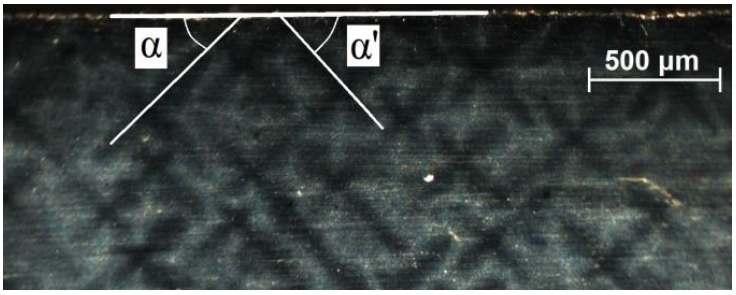

Figure 1. Graphical depiction of the angles used to approximate CMSX-4 sample's crystalline orientations

From Figure 1, α and α' are the angles that the dendrite's secondary arms form relative to the substrate larger surface. α is always considered to be the smallest angle from both. The measurement of α was manually made five times per sample in different locations of the exposed surface utilizing an image measurement software (Datinf®Measure). The average from these values was taken as the sample's α. Finally, every sample with α smaller or equal to 10° was considered to have its testing surface "parallel" to the (010) plane, and therefore, being suitable for testing. The tolerances were defined based on an approximated angle variation at which different microstructural results or defects start to be relevant to the process (Mokadem et al., 2007; Wang et al., 2015, 2004). For further reference a 10° tolerance around each axis was taken as acceptable. The CMSX-4 powder particle diameter used in the cladding process ranged between 25 and 75 μm.

2.1. Single Track Clads – Definition and measurement

A single clad track is the deposition formed by a single pass of the cladding head. On this work, only straight tracks were done. All tracks and remelting experiments had the laser and powder focal points at sample surface. Also, the cladding and laser axis were always maintained perpendicular to the worked surface.

A straight forward parameter study was used to define five clad tracks that would be used in the further tests. This number was defined according to the number of available samples. Only one of the three main cladding parameters (laser power, traverse speed and powder feeding rate) (Kaierle et al., 2012) was varied per test. Tendencies on resultant geometry and microstructure were followed until the final tracks were defined. No deep perfecting of cladding parameters was done, once that non-optimal clads could even help proving the efficacy of the remelting technic. The tracks that were considered candidates to be used for further testing had to meet two conditions, the material deposition had not to diminish substrate single crystallinity, at least in a first evaluation, and the track needed to present absence of cracks and pores.

At this first batch of tests, the transversal section of the tracks was evaluated only once. Metallographic data, which was to be used to compare the tracks, was acquired by measuring microstructural distances. The measures taken were: (i) clad height, *h*, measured here as the height from the substrate surface to the clad highest point; (ii) clad width, *w*, measured as the material deposition's width at substrate surface level; (iii) melt pool depth, *h'*, considered to be the longer height found from the substrate surface to the bottom of the melt pool planar grown region; (iv) track SX-height, h_{sx}, as the shortest distance from the sample surface to misorientation beginning.

Once the five final tracks were chosen, they had their characterization reviewed and reinforced. Two more transversal metallographies and one longitudinal were done for each final track to gather averages. *h'* values were acquired in three locations of the longitudinal sections, then averaged together with the ones measured in the transversal sections, therefore defining its final values. The final h_{sx} values were considered to be the smallest SX-heights found for each track in all sections. Clad height was redefined as the middle point between the clad highest and lowest points found. Final *w* values could only be taken from a track's transversal section and were taken as the averages from their measurements. All the data acquisition was done inside the tracks' geometrically constant section, disregarding start and end regions.

2.2. Remelting Tests

Remelting of SX Ni-based superalloys can form SX-microstructure (Liu, 2014). Here it was used as a way of extending the overall SX-height in a clad track by re-solidifying its misoriented region. Once the laser beam geometry and energy distribution pattern is fixed, the laser remelting process is mainly controlled by two variables, laser power and traverse speed, being it a simpler process when compared to laser cladding. The laser power in the remelting tests was theoretically limited by the range of laser powers and the speeds used to form the clads themselves. Within this range, the amount of energy per volume used to form a complete clad will be higher than the necessary to melt a part of it. Therefore, for each final clad track there were specific limiting remelting power and speed values. Remelting parameters were ranged around such energy input values, being such values calculated through the following formula.

$$E_{St} = \frac{P_L}{V} \tag{1}$$

Were E_{St} is the energy input per millimetre, P_L is laser power and V is traverse speed (Kaierle et al., 2012). Clads of different shapes were used to explicit different laser remelting characteristics. The characteristics are listed in the results through macro- and micrographies. Remelting speeds ranged from 1,7 mm/s to 3,3 mm/s and P_L was varied between 68 W and 189 W.

One combination of remelting and clad results was chosen to be used in the multi-layer clads. Its resultant misoriented height had to be smaller than h' so that the undesired microstructure could be completely remolten in the layer to come. The tracks' remelting was performed with constant speed, being laser power raised to plateau and decreased one millimetre after and before the clad line. However, before moving to such clads, the spacing between tracks and the cladding strategy had to be defined.

2.3. Initial Multi-Layer Cladding Strategy

Substrate orientation and heat drainage effects must be considered when defining cladding strategies, especially when intending to construct a SX clad tracks-wide and layers-high. Therefore, once the samples used had always the main crystalline direction perpendicular to the worked surface, it is of interest to align the heat flow from the melt pool to this direction, thus, retarding the OMT and reducing stray grain formation. The most common cladding strategy used to mount a clad layer is to directly overlap part of the previous track with the next one. This results in non-beneficial effects to the crystalline orientation in question since the new track's melt pool's heat would be drained between the previous track and the substrate, partially misaligning the thermal gradient. Besides, the second track surface would form a relatively acute angle to the substrate, which could come to result in pore formation and cracks; especially when working with CMSX-4 (Schweitzer, 2015). The solution proposed was to clad two tracks with a gap between them and then fill this space with a third track. With this displacement, the two base tracks would transfer the heat gained straight to the substrate, while the middle one would have its maximal misoriented heat gradient decreased, once its heat volume – which is still is the same quantity as before – is now divided to another direction symmetrically positioned. Always placing tracks separately and they filling the space between it and the rest of the layer would repeat this heat drainage conditions. The surface angle problem would also be solved by this method, once no acute angle is formed.

To define the spacing between tracks (s), a simple approach considering the chosen track's transversal section and an overlapping factor (o) was designed, Fig. 2. It affirms that the area between consecutive base tracks should be close to the chosen track's area above substrate surface (A_t). In the approach, A_t is subtracted from the area formed by multiplying w and h. This calculates the transversal area to be filled above the two base tracks (A_f). The remaining of the gap is a square shaped area within tracks (A_s) delimited by the sample surface and h. Its size is given by subtracting A_f from A_t, and since its height is equal to h, its width (w_s) is promptly defined. With w_s calculated, the initial o, o_i, is determined through:

$$o = \frac{(w_s + w)}{w} \tag{2}$$

And with o_i and w, the initial spacing is defined using:

$$s = o * w \tag{3}$$

As can be seen o defines s based on w, being, therefore, the variable. The calculated o_i was used to determine the first condition at which the triple clad could form a proper pattern to be repeated. However, o_i is just an initial approximation; it is not guaranteed that this is a suitable value for o, once powder deposition shan't occur in the same amount between a flat surface and a gap. Thus, other two o values near o_i were applied to test such patterns. A graphical representation of the measures mentioned before is disposed in Fig. 2.

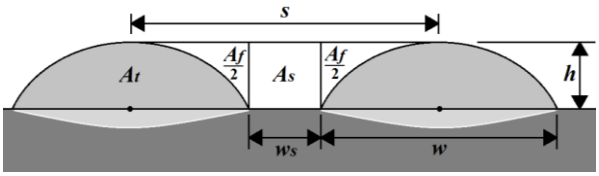

Figure 2. Geometrical relations used to determine multi-layer cladding pattern

After the pattern was decided, the first multi-layer clad was executed by repeating this pattern horizontally until seven tracks were laid. Cladding head was then moved up the length of an h in height and an identic layer was executed; a total of four layers were done per clad. In layer formation all base track were deposited, then the gaps between them were filled. Clad and remelting passes were executed in the same direction. The tracks had approximately five millimetres in length. From one pass to the next one, be it of remelting or cladding, a pause was made with intent to let the sample return to room temperature, thus, providing similar solidification conditions for all tracks. To evaluate layer patterns and multi-layer clad strategies top macrographs and transversal section metallographies were taken.

3. RESULTS AND DISCUSSION

3.1 Single Track Clads

The cladding parameter study concluded in the five final tracks that gave work material to the remelting tests. These track's cladding parameters, powder feeding rate ($\dot{m}$), laser power (P_L) and cladding speed (V_c), are listed – on Tab. (1).

Table 1. Final tracks' cladding parameters

	P1	P2	P3	P4	P5
$\dot{m}$ (g s-1)	3.0	1.5	1.5	2.5	1.0
P_L (W)	100	100	100	200	100
V_c (mm s-1)	0.5	0.5	1.0	1.7	1.0

In Table (2), their h_{sx} values are expressed individually in those extracted only from a single transversal section – to decide which tracks would be used – and those that additionally considered the two subsequent traversal sections and the longitudinal one used to reinforce measurements.

Table 2. Final tracks' h_{sx} values measured for final track definition and after their definition.

	P1	P2	P3	P4	P5
1st acquisition (μm)	204	181	55	132	21
Complete acquisition (μm)	183	49	-23	21	-35

These results prove that h_{sx} should not only be measured from transversal sections, but from longitudinal sections also, or at least, in more points through the clad. This is because some clad parameters cause inconstant crystallinity heights along the clad's longitudinal axis, therefore, giving false h_{sx} values. The phenomenon could be explained by melt pool chemical composition variations or simply through process instabilities. However, when working with approximated crystalline directions, one can also expect that h_{sx} results could differ considerably from one sample to another; therefore, more measurements are indeed required. The final values of the properties measured, rather than only h_{sx}, for each final track are displayed on Tab. (3).

Table 3. Final tracks' properties measured

	h(μm)	w (μm)	h' (μm)	h_{sx} (μm)	A_p (μm²)
P1	792	590	92	183	364100
P2	451	781	98	49	238800
P3	223	842	132	-23	135600
P4	415	1068	162	21	313100
P5	181	849	151	-35	134500

With the final tracks defined and measured, the experimentation continued to the remelting tests.

3.2. Remelting Results

The first effect noticed on the remelting pass is the homogenization and levelling of the cladded track's surface. During cladding the powder particles may not be completely melted, leaving a rough surface that can affect the next clad to come. In Fig. 3, the two top view of two depositions are depicted; (a) is P5 without remelting, (b) is the same parameter after being remolten. One can see the reduction in half-molten particle from the left picture to the right one.

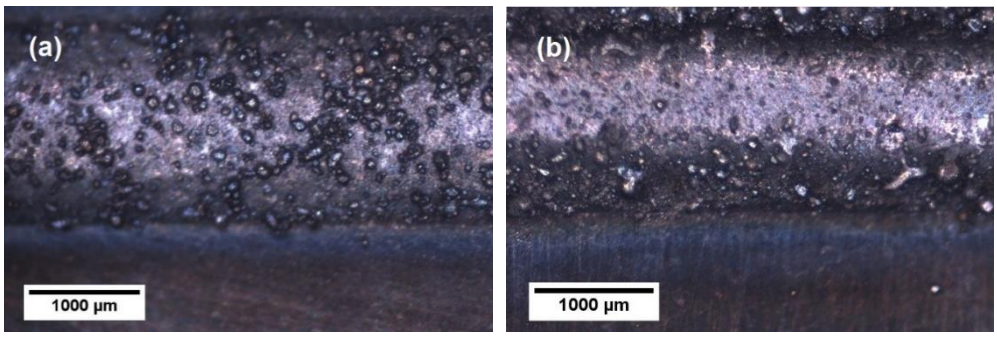

Figure 3. Top view of un-remolten clad track over substrate (a). Remolten clad track (b), decrease in surface roughness is visible.

In sequence two longitudinal micrographies of P1 are exposed in order to evidence two effects originated from laser remelting, Fig. 4. They are the levelling of the clad's surface and the forecasted SX extension. The levelling can be seen from the un-remolten clad track to the remolten one, Fig. 4.a and Fig. 4.b, respectively. It can ease further cladding depositions, once that the material to be deposited will be laid over a more even surface. The SX extension is proven through the Fig. 4.b, by the well oriented dendrites present over the white planar grown region line caused by the remelting. This line also represents the depth limit at which the clad was remolten.

The dendrites can only be observed because the grown dendrites' main branches are parallel to the plane of visualisation. They can be spotted as the white line perpendicular to both planar grown regions. The volume present above the dendrites is what was called the misoriented volume, and as can be seen, it remains present even after the laser remelting pass. The complete suppression of this problem was not possible in this work's batch of tests, although its gravity was mitigated.

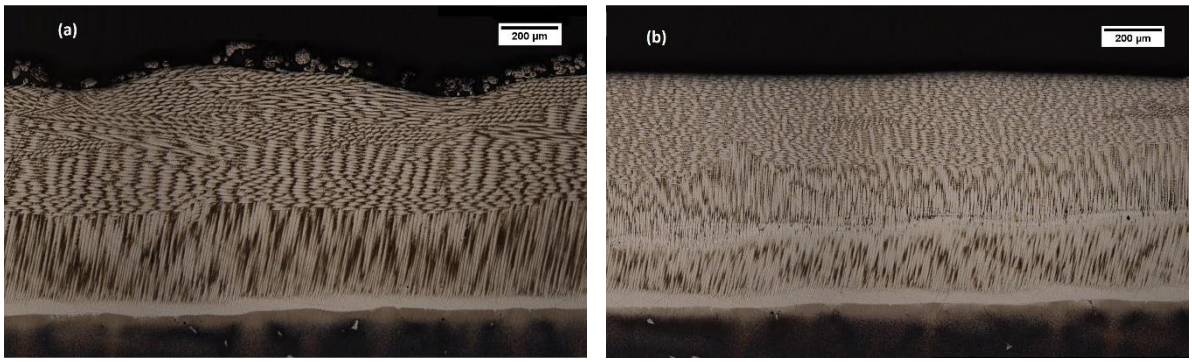

Figure 4. Longitudinal micrograph of un-remolten clad track (a). Remolten clad track (b), levelling of top surface and increase in single crystallinity.

As for transversal evaluation of laser remelted clads, considerations are made over the next micrographies. The image on the left shows un-remelted clads, while the image on the right shows their respective remolten tracks. On Fig. 5, P1, the highest clad track chosen, is depicted. It can be seen, that before remelting it already has a negative interface angle with the substrate, feature that is aggravated after remelting. This happens because the clad's upper material has a second chance to flow down, flattening the cladded track. Such resultant transversal shape does not favour lateral overlapping, only vertical superposition, being useful only when the intention is to build a "wall" instead of a layer. Since this is not the case in question, the parameter P1 with its remelting parameters was discarded as an option for the multi-layer cladding. However, it demonstrated a different aspect of laser remelting.

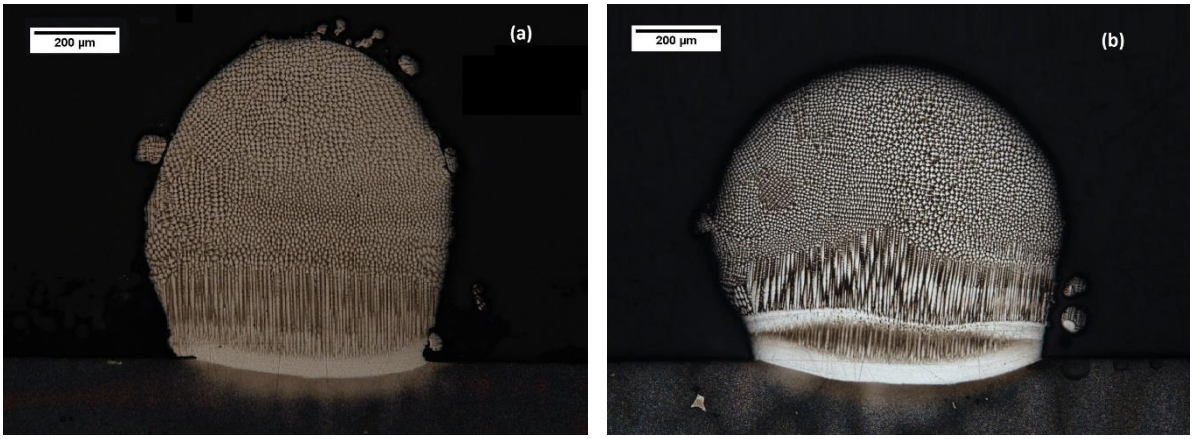

Figure 5. Transversal micrograph of un-remolten P1 clad track over substrate (a). Remolten P1 clad track (b), deformation of original shape is evident.

For the parameter P2, P3 and P4 proper remelting parameters could not be found. In this work's initial study of the remelting process, their related remelting parameters did resulted in higher single crystallinities, but the resultant SX increase did not reached useful heights. Only cladding parameter P5 and its depicted remelting, Fig. 6, reached the condition were the misoriented volume's height was lower than h'.

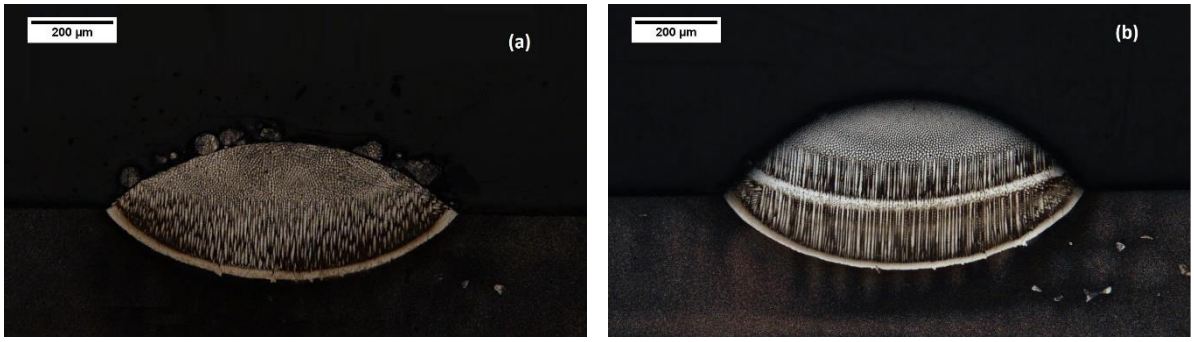

Figure 6. Transversal micrograph of un-remolten P5 clad track over substrate (a). Remolten P5 clad track (b), speed chosen of 3.3 mm·s-1 and laser power 70 W. Remelting result provided proper track for superposition.

Therefore, as mentioned, with P5, the single crystallinity seems to have been extended over to useful heights. The uncertainty in these affirmation is only due the fact that these properties were not measured according to the methods mentioned in the experimental section, which consider process instabilities, and were measured only once in a transversal metallography. Nevertheless, the tests continued to multi-layer cladding where these specific cladding and remelting parameters were to be repeated and their stability confirmed.

3.3. SX Multi-Layer Clad

On the multi-layer cladding, three pattern spacing were tested. One was based on the calculation done and had o_i equal to 1.7 and the two other overlapping had o equal to 1.5 and 1.3. These patterns used the P5 cladding parameter together with its optimal remelting at 3.3 mm·s-1 and 70W. The resultant three-line clads are depicted in Fig. 7.

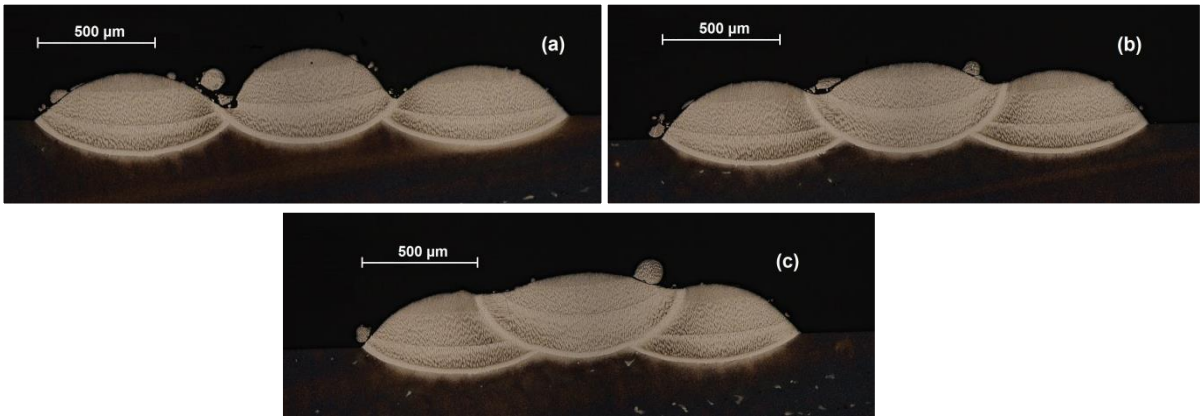

Figure 7. Multi-layer cladding patterns tested

The spacing that gave best results was the one with *o* equal to 1.3, Fig. 7.c. Other than its correlatives, it presented no lack of filling as the one in Fig. 7.a, or low misorientation within tracks as in *o* equal to 1.5 – Fig. 7.b. The misorientation of Fig. 7.b is detailed in Fig. 8.

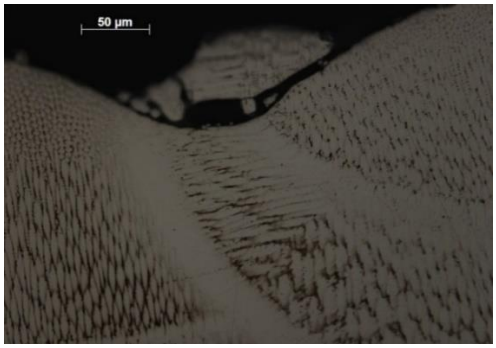

Figure 8. Possible misorientation within the patterns' tracks

It can be said that the small dendrites grown horizontally could be well oriented, with no high angle grain boundary existing between them and the ones growing form the melt pool's bottom. However, the region within the two front is ought to be tensioned due to its susceptibility to hot cracking (Wang et al., 2004), therefore, on this basis, it was preferred to choose for a smaller spacing were this region is more likely to be re-molten by the next layer.

With the pattern defined, the multi-layer clad strategy described in the experimental section was performed. Its complete metallography is shown in Fig. 9.a and details from such are present in Fig. 9.b and 9.c.

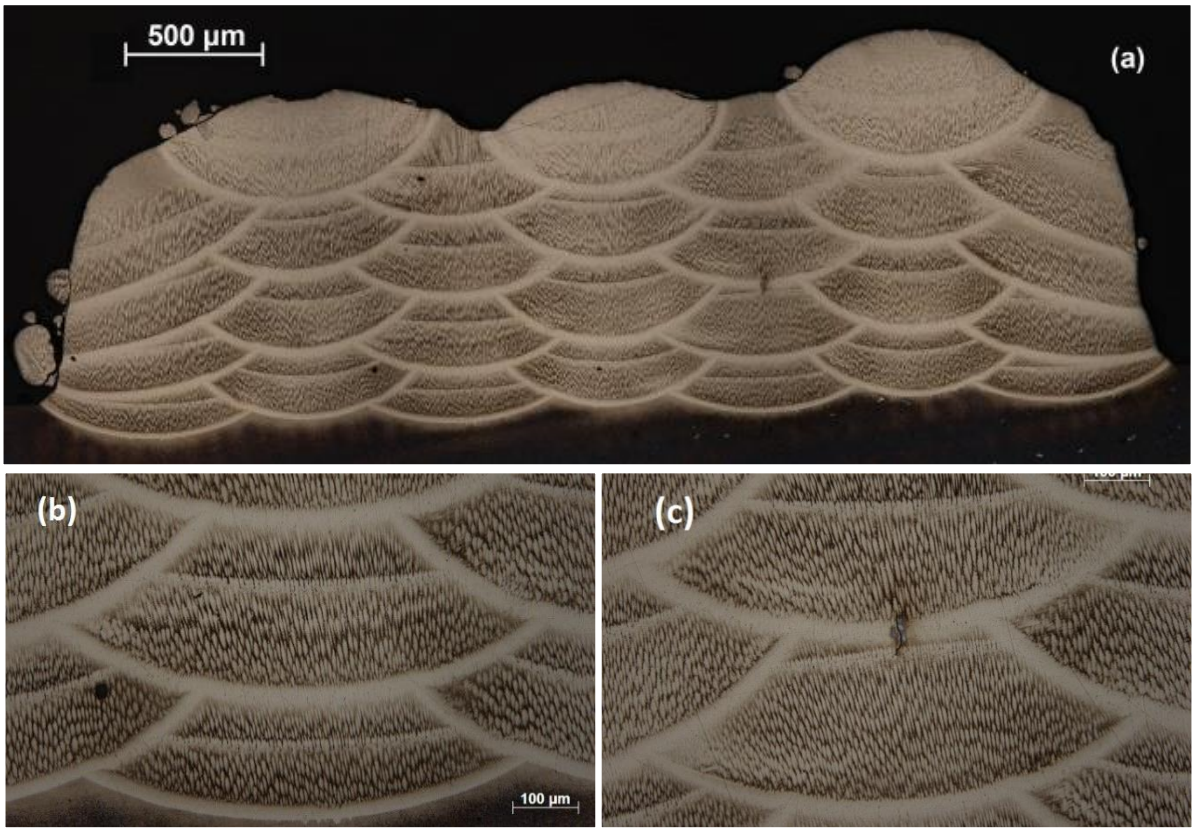

Figure 9. CMSX-4 multi-layer clad and its microstructural defects, remelting passes performed at 3.3 mm·s-1

The resultant clad demonstrated in its transversal section is a single crystalline deposition of approximately 3700 µm in width and 650 µm in height, as all of its grow dendrites are pointed in the same direction. Its planar grown regions created by the remelting passes presented a slight increase in the distance from their respective track's planar grown regions as the measure moved upwards, Fig. 9.b. This implied that the height layer step should be slightly adjusted from *h*, not directly taken, as supposed. This discrepancy is probably due to the small hump in the middle of the pattern chosen, which could have increased layer height from h. In Fig. 9, it can also be seen that the misoriented regions, exemplified in Fig. 8, were completely supressed.

The other imperfection found, on Fig. 9.c, suggested that a crack was originated from the remelting pass and that it was deep enough to not be molten by the next clad pass. As last remark over this strategy is that it could be extended through the three axes, possibly generating even larger SX depositions if solidification conditions were maintained.

4. CONCLUSION

Laser re-melting for track single crystallinity extension proved itself a tool capable of improving and simplifying the formation of large SX-volumes by laser powder cladding, and possibly of other similar processes. The experiments exposed aspects of laser re-melting that can be used – or should be accounted for – when attempting the repair of SX-Ni-based superalloy turbine blades. Further development of this process can bring researches one step closer to achieving a reliable repair process for such SX-superalloys. The multi-layer SX clad deposition presented should be repeated and evaluated with more precise technics, such as Electron Back Scatter Diffraction (EBSD), to fully confirm its single crystallinity, however results are promising. A possibility to be analysed in future experiments is to evaluate the relief of tensions caused by the laser remelting on the under laid clads, a possible beneficial phenomenon of this process.

5. ACKNOLEGMENTS

The work presented was supported by the German Research Foundation (DFG) within the scope of the sub-project B5 “Single crystalline laser cladding” of the Collaborative Research Centre (SFB 871 "Product Regeneration"). Thanks go to the DFG for their support**.**

The authors also thank the support of the Laboratório de Mecânica de Precisão (LMP – LASER) from the Universidade Federal de Santa Catarina (UFSC).

6. REFERENCES

Acharya, R., Bansal, R., Gambone, J.J. and Das, S. (2014a), “A Coupled Thermal, Fluid Flow, and Solidification Model for the Processing of Single-Crystal Alloy CMSX-4 Through Scanning Laser Epitaxy for Turbine Engine Hot-Section Component Repair (Part I)”, *Metallurgical and Materials Transactions B*, Vol. 45 No. 6, pp. 2247–2261.

Acharya, R., Bansal, R., Gambone, J.J. and Das, S. (2014b), “A Microstructure Evolution Model for the Processing of Single-Crystal Alloy CMSX-4 Through Scanning Laser Epitaxy for Turbine Engine Hot-Section Component Repair (Part II)”, *Metallurgical and Materials Transactions B*, Vol. 45 No. 6, pp. 2279–2290.

Gäumann, M., Bezençon, C., Canalis, P. and Kurz, W. (2001), “Single-crystal laser deposition of superalloys: Processing-microstructure maps”, *Acta Materialia*, Vol. 49 No. 6, pp. 1051–1062.

Gäumann, M., Trivedi, R. and Kurz, W. (1997), “Nucleation ahead of the advancing interface in directional solidification”, *Materials Science and Engineering: A*, Vol. 226–228, pp. 763–769.

Hunt, J.D. (1984), “Steady state columnar and equiaxed growth of dendrites and eutectic”, *Materials Science and Engineering*, Vol. 65 No. 1, pp. 75–83.

Kaierle, S., Barroi, A., Noelke, C., Hermsdorf, J., Overmeyer, L. and Haferkamp, H. (2012), “Review on Laser Deposition Welding: From Micro to Macro”, *Physics Procedia*, Vol. 39, pp. 336–345.

Liu, W. and DuPont, J.N. (2004), “Effects of melt-pool geometry on crystal growth and microstructure development in laser surface-melted superalloy single crystals”, *Acta Materialia*, Vol. 52 No. 16, pp. 4833–4847.

Liu, W. and DuPont, J.N. (2005), “Effects of substrate crystallographic orientations on crystal growth and microstructure development in laser surface-melted superalloy single crystals. Mathematical modeling of single-crystal growth in a melt pool (Part II)”, *Acta Materialia*, Vol. 53 No. 5, pp. 1545–1558.

Liu, X. (2014), “Entwicklung eines einkristallinen Laser-Umschmelz- Prozesses für die Nickelbasis-Superlegierung CMSX-4 zur Wiederherstellung von Defekten an einkristallinen Bauteilen orthogonal zur Erstarrungsrichtung”.

Liu, Z. and Qi, H. (2014), “Numerical simulation of transport phenomena for a double-layer laser powder deposition of single-crystal superalloy”, Vol. 45 No. April, pp. 1903–1915.

Liu, Z. and Qi, H. (2015), “Effects of substrate crystallographic orientations on crystal growth and microstructure formation in laser powder deposition of nickel-based superalloy”, *Acta Materialia*, Vol. 87, pp. 248–258.

Liu, Z., Qi, H. and Jiang, L. (2016), “Control of crystal orientation and continuous growth through inclination of coaxial nozzle in laser powder deposition of single-crystal superalloy”, Vol. 230, pp. 177–186.

Mokadem, S., Bezençon, C., Hauert, a., Jacot, A. and Kurz, W. (2007), “Laser repair of superalloy single crystals with varying substrate orientations”, *Metallurgical and Materials Transactions A: Physical Metallurgy and Materials Science*, Vol. 38 A No. 7, pp. 1500–1510.

Schweitzer, L. (2015), “Laser Cladding for Epitaxial Nickel Base Superalloys Turbine Blades”.

Vitek, J.M. (2005), “The effect of welding conditions on stray grain formation in single crystal welds - Theoretical analysis”, *Acta Materialia*, Vol. 53 No. 1, pp. 53–67.

Wang, L. and Wang, N. (2016), “Effect of substrate orientation on the formation of equiaxed stray grains in laser surface remelted single crystal superalloys : Experimental investigation”, Vol. 104, pp. 250–258.

Wang, L., Wang, N., Yao, W.J. and Zheng, Y.P. (2015), “Effect of substrate orientation on the columnar-to-equiaxed transition in laser surface remelted single crystal superalloys”, *Acta Materialia*, Acta Materialia Inc., Vol. 88, pp. 283–292.

Wang, N., Mokadem, S., Rappaz, M. and Kurz, W. (2004), “Solidification cracking of superalloy single- and bi-crystals”, *Acta Materialia*, Vol. 52, pp. 3173–3182.

7. RESPONSIBILITY NOTICE

The authors are the only responsible for the printed material included in this paper.